Water Research 206 (2021) 117673

Contents lists available at ScienceDirect

Water Research

journal homepage: www.elsevier.com/locate/watres

Importance of thermodynamics dependent kinetic parameters in nitrate-based souring mitigation studies

Moein Jahanbani Veshareh [a,*], Jan Dolfing [b], Hamidreza M. Nick [a]

[a] Danish Hydrocarbon Research and Technology Centre, Technical University of Denmark, Lyngby, Denmark
[b] Faculty of Engineering and Environment, Northumbria University, Newcastle upon Tyne, UK

ARTICLE INFO

Keywords:
Modeling
souring
nitrate treatment
thermodynamics
Gibbs energy

ABSTRACT

Souring is the unwanted formation of hydrogen sulfide (H_2S) by sulfate-reducing microorganisms (SRM) in sewer systems and seawater flooded oil reservoirs. Nitrate treatment (NT) is one of the major methods to alleviate souring: The mechanism of souring remediation by NT is stimulation of nitrate reducing microorganisms (NRM) that depending on the nitrate reduction pathway can outcompete SRM for common electron donors, or oxidize sulfide to sulfate. However, some nitrate reduction pathways may challenge the efficacy of NT. Therefore, a precise understanding of souring rate, nitrate reduction rate and pathways is crucial for efficient souring management. Here, we investigate the necessity of incorporating two thermodynamic dependent kinetic parameters, namely, the growth yield (Y), and F_T, a parameter related to the minimum catabolic energy production required by cells to utilize a given catabolic reaction. We first show that depending on physiochemical conditions, Y and F_T for SRM change significantly in the range of [0-0.4] mole biomass per mole electron donor and [0.0006-0.5], respectively, suggesting that these parameters should not be considered constant and that it is important to couple souring models with thermodynamic models. Then, we highlight this further by showing an experimental dataset that can be modeled very well by considering variable F_T. Next, we show that nitrate based lithotrophic sulfide oxidation to sulfate ($lNRM_3$) is the dominant nitrate reduction pathway. Then, arguing that thermodynamics would suggest that S° consumption should proceed faster than S^0 production, we infer that the reason for frequently observed S^0 accumulation is its low solubility. Last, we suggest that nitrate based souring treatment will suffer less from S^0 accumulation if we (i) act early, (ii) increase temperature and (iii) supplement stoichiometrically sufficient nitrate.

Abbreviations

SRM	sulfate reducing microorganisms
oNRM	organotrophic nitrate reducing microorganisms
lNRM	lithotrophic nitrate reducing microorganisms
laNRM	lithoautotrophic nitrate reducing microorganisms
lhNRM	lithoheterotrophic nitrate reducing microorganisms
$laNRM_1$	lithoautotrophic nitrate reducing sulfide oxidizing to sulfur microorganisms
$laNRM_2$	lithoautotrophic nitrate reducing sulfur oxidizing to sulfate microorganisms
$laNRM_3$	lithoautotrophic nitrate reducing sulfide oxidizing to sulfate microorganisms
$lhNRM_1$	lithoheterotrophic nitrate reducing sulfide oxidizing to sulfur microorganisms
$lhNRM_2$	lithoheterotrophic nitrate reducing sulfur oxidizing to sulfate microorganisms
$lhNRM_3$	lithoheterotrophic nitrate reducing sulfide oxidizing to sulfate microorganisms
$lNRM_1$	lithotrophic nitrate reducing sulfide oxidizing to sulfur microorganisms
$lNRM_2$	lithotrophic nitrate reducing sulfur oxidizing to sulfate microorganisms
$lNRM_3$	lithotrophic nitrate reducing sulfide oxidizing to sulfate microorganisms
ED	electron donor
EA	electron acceptor
NT	nitrate treatment

* Corresponding author.
E-mail address: moein@dtu.dk (M.J. Veshareh).

https://doi.org/10.1016/j.watres.2021.117673
Received 10 May 2021; Received in revised form 30 August 2021; Accepted 15 September 2021
Available online 21 September 2021

1. Introduction

Biologic hydrogen sulfide (H_2S) production due to the activity of sulfate reducing microorganisms (SRM), or the so-called souring process, is a common problem in sewer systems (Jiang et al., 2014) and secondary oil recovery by seawater flooding (Veshareh and Ayatollahi, 2019) due to the odorant, corrosive and toxic nature of H_2S. Nitrate treatment (NT) is one of the intervention methods to control souring by stimulating nitrate reducing microorganisms (An et al., 2010). Nitrate can suppress souring by various mechanisms such as activating organotrophic nitrate-reducing microorganisms (oNRM) that may outcompete SRM for the available organic matter (Agrawal et al., 2012), and reducing sulfide concentration by stimulating lithotrophic nitrate-reducing microorganisms (lNRM) (Veshareh et al., 2021). Lithotrophic nitrate-reduction based sulfide-oxidation can be associated with biogenic elemental sulfur (S^0) (Huang et al., 2015). Due to the corrosive character of S^0 (Lahme et al., 2019; Schmitt, 1991), its accumulation can reduce the efficiency of NT (Dolfing and Hubert, 2017). Therefore, an understanding of likely nitrate reduction pathways as well as kinetics of sulfate and nitrate reduction is essential for designing promising NT plans.

Respiring prokaryotes catalyze redox reactions (called catabolic reactions) to derive energy for growth and maintenance (Jin, 2012). The amount of free energy available from various redox reactions, or Gibbs free energy of catabolic reaction (ΔG_{cat}) has been used by scientists as a method to compare the likelihood of different metabolisms/pathways. For example, Dolfing and Hubert (2017) used this method to predict nitrate reduction pathways in nitrate-based oil reservoir souring mitigation. Since under typical oil reservoir conditions $-\Delta G_{cat}$ of nitrate reduction coupled to acetate oxidation was higher than nitrate reduction coupled to sulfide oxidation, they proposed that under realistic oil field conditions nitrate reduction is more likely to be organotrophic rather than lithotrophic. Dolfing and Hubert (2017) claimed that lithotrophic nitrate reduction coupled to partial oxidation of sulfide to sulfur is an exception and can be more favorable than organotrophic nitrate reduction as far as acetate to sulfide molar ratio is less than 0.001, or the temperature is sufficiently low. Additionally, showing that per mole of nitrate sulfide oxidation to S^0 releases slightly more energy than sulfide oxidation to sulfate, they suggested that S^0 accumulation is likely to occur under nitrate limiting conditions. The assessment of Dolfing and Hubert labels one metabolism/pathway as favorable and the other as unfavorable, and does not allow an energy based quantitative comparison between the occurrence likelihood of each metabolism. We are not aware of any previous research that has used thermodynamics to make a quantitative comparison between the occurrence likelihood of various nitrate reduction pathways in presence of sulfide and S^0. However, for some other metabolisms such as syntrophic oxidation, iron reduction, sulfate reduction and methanogenesis, Jin and Kirk (2016) and Jin and Kirk (2018) used a thermodynamic limiting factor (F_T) that relates the rate of microbial metabolisms to ΔG_{cat}. The F_T coefficient is not the only term that links thermodynamics to metabolism kinetics. Growth yield (Y) is another parameter that controls the kinetics of microbial metabolisms and is a function of ΔG_{cat} and of the Gibbs free energy of anabolic reaction (ΔG_{an}) (Jin and Roden, 2011; Smeaton and Van Cappellen, 2018). To the best of our knowledge, no previous research work has used growth yield to relate thermodynamics of microbial reactions to their kinetics. Note that Y and F_T have been assumed to be constant in biomass explicit microbial kinetic models used over the last decades to simulate souring and its mitigation with nitrate (Hvitved-Jacobsen et al., 2013; Sharma et al., 2008; Veshareh and Nick, 2019, 2021a; 2021b). As such, the error associated with assuming Y and F_T parameters to be constant in simulation of souring process and nitrate-based souring mitigation measures, is unknown.

To address the abovementioned gaps, in this article, we calculate Y and F_T to evaluate the range in which they vary under various physiochemical conditions such as electron donor (ED) and electron acceptor (EA) availability, pH and temperature, relevant to sewer systems and petroleum reservoirs. We then use Y to link thermodynamics of sulfur and nitrogen cycle to their kinetics. Using this link, we first revisit the questions raised by Dolfing and Hubert (2017) by illuminating whether nitrate reduction is more likely to be organotrophic or lithotrophic, and whether or not S^0 accumulation during NT is due to a thermodynamic drive. Lastly, we suggest some measures to minimize S^0 accumulation in NT of souring.

2. Theory

Lithotrophic nitrate reducers can obtain their energy by (i) oxidation of sulfide to sulfur ($lNRM_1$), (ii) oxidation of sulfur to sulfate ($lNRM_2$) and (iii) direct oxidation of sulfide to sulfate ($lNRM_3$). Regardless of whether nitrate is reduced through lNRM or oNRM, it is reduced either to nitrogen gases through denitrification or to ammonium through dissimilatory nitrate reduction (DNRA) (Callbeck et al., 2013). However, various research works (e.g. (Veshareh and Nick, 2019) and (Marietou et al., 2020)) have shown that DNRA is the responsible nitrate reduction pathway in nitrate mitigation of reservoir souring. Therefore, here we do not consider redox reactions related to the denitrification pathway. Lithotrophic nitrate-reducing microorganisms can be autotrophic (laNRM) (Hamilton et al., 2015) or heterotrophic (lhNRM) (Miroshnichenko et al., 2003). Various organic compounds can serve as the ED of SRM and oNRM; however, Dolfing and Hubert (2017) showed that the energy yield of SRM and oNRM metabolisms is independent of the type of the organic ED used. Therefore, here we only consider acetate as the ED, and as the organic carbon source for cell synthesis of organotrophic and lithoheterotrophic metabolisms. Catabolic and anabolic reactions are from, or are based on the methodology introduced by Smeaton and Van Cappellen (2018). Table 1 and 2 list the catabolic and anabolic reactions that represent various metabolisms studied in this work.

Chemical compounds in the aqueous phase can lose or obtain protons or hydroxide due to reaction with water molecules, or combine with other ions or molecules in a process called speciation (Jin and Kirk, 2018). Due to speciation, chemical compounds dissolved in water can exist in various forms or chemical species. As a result, environmental pH can affect the energetics of redox reactions directly by changing the chemical activity of protons, for redox reactions that consume or produce protons, or indirectly, by controlling the speciation of reactants and products. In this work, all reactions are written using dominant chemical species at pH 7. At a neutral pH, hydrogen sulfide (HS^-) occurs in relatively equal proportions as dihydrogen sulfide (H_2S). Following Smeaton and Van Cappellen (2018), we choose HS^-. Catabolic and anabolic reactions are written per mole ED and per mole biomass,

Table 1
The catabolic and anabolic reaction, Gibbs free energy and enthalpy for various metabolisms studied in this work.

Metabolism	Reaction type	Reaction number
oSRM	Catabolic	1
	Anabolic	2
oNRM	Catabolic	3
	Anabolic	2
$lhNRM_1$	Catabolic	4
	Anabolic	2
$lhNRM_2$	Catabolic	5
	Anabolic	2
$lhNRM_3$	Catabolic	6
	Anabolic	2
$laNRM_1$	Catabolic	4
	Anabolic	7
$laNRM_2$	Catabolic	5
	Anabolic	8
$laNRM_3$	Catabolic	6
	Anabolic	9

Table 2
Catabolic and anabolic reactions corresponding to various metabolisms and pathways listed in Table 1.

Reaction number	Reaction	$\Delta G^{\circ}_{298.15}$(*)	$\Delta H^{\circ}_{298.15}$(*)
1	$C_2H_3O_2^- + SO_4^{2-} \rightarrow 2\ HCO_3^- + HS^-$	-48.13	-0.3598
2	$0.525\ C_2H_3O_2^- + 0.2\ NH_4^+ + 0.275\ H^+ \rightarrow CH_{1.8}O_{0.5}N_{0.2} + 0.05\ HCO_3^- + 0.4\ H_2O$	18.64	41.61
3	$C_2H_3O_2^- + H_2O + H^+ + NO_3^- \rightarrow NH_4^+ + 2\ HCO_3^-$	-536.0	-534.5
4	$HS^- + 1.5\ H^+ + 0.25\ NO_3^- \rightarrow 0.25\ NH_4^+ + S + 0.75\ H_2O$	-182.0	-180.0
5	$S + 1.75\ H_2O + 0.75\ NO_3^- \rightarrow 0.75\ NH_4^+ + SO_4^{2-} + 0.5H^+$	-305.9	-354.3
6	$HS^- + H_2O + H^+ + NO_3^- \rightarrow NH_4^+ + SO_4^{2-}$	-487.9	-534.2
7	$HCO_3^- + 2.1\ HS^- + 0.2\ NH_4^+ + 2.9\ H^+ \rightarrow CH_{1.8}O_{0.5}N_{0.2} + 2.1\ S + 2.5\ H_2O$	-82.09	-55.48
8	$HCO_3^- + 0.7\ S + 0.2\ NH_4^+ + 0.3\ H_2O \rightarrow CH_{1.8}O_{0.5}N_{0.2} + 0.7\ SO_4^{2-} + 0.6\ H^+$	85.90	74.22
9	$HCO_3^- + 0.525\ HS^- + 0.2\ NH_4^+ + 0.275\ H^+ \rightarrow CH_{1.8}O_{0.5}N_{0.2} + 0.525\ SO_4^{2-} + 0.4\ H_2O$	43.91	41.80

*kJ/mol ED for catabolic reaction and kJ/c-mol biomass for anabolic reaction

respectively.

3. Methodology

According to the thermodynamically consistent rate law (Jin and Bethke, 2005; 2007), respiration rate (r) [mol ED·s^{-1}] can be written as follows:

$$r = v_{max}\ X\ F_K\ F_T \tag{1}$$

where v_{max} [mol ED · (mol biomass)$^{-1}$· s^{-1}] is the maximum rate of a metabolism, X is the biomass concentration [mol · (kg water)$^{-1}$], F_K is a kinetic limiting term and F_T is a thermodynamic limiting term. According to Monod (1949) and LaRowe et al. (2014) F_K and F_T can be defined as follows:

$$F_K = \frac{C_{ED}}{K_{ED} + C_{ED}} \frac{C_{EA}}{K_{EA} + C_{EA}} \tag{2}$$

$$F_T = \begin{cases} \dfrac{1}{\exp\left(\dfrac{\Delta G_{cat} + F\Delta\psi}{RT}\right) + 1} & \text{for } \Delta G_{cat} \leq 0 \\ 0 \text{ for } \Delta G_{cat} \geq 0 \end{cases} \tag{3}$$

Where C [mol · (kg water)$^{-1}$] is concentration, K is half saturation constant, ΔG_{cat} [J· (mol e^-)$^{-1}$] is the Gibbs free energy of a metabolism's catabolic reaction under non-standard conditions, F [C · mol^{-1}] is the Faraday constant, R [J · mol^{-1} · K^{-1}] is the gas constant, T [K^{-1}] is temperature, and $\Delta\psi$ [V] is the electric potential across the membrane. The subscripts ED and EA denote electron donor and electron acceptor, respectively. Even though the value of $\Delta\psi$ can be different for various low energy environments and for various metabolisms, an evaluation of investigations on several distinct organisms led to the proposition that 120 mV can be considered a representative value for $\Delta\psi$ (Dimroth et al., 2003; Kadenbach, 2003). Toei et al. (2007) and Daniels et al. (1984) reported a value of 118 mV for $\Delta\psi$. Therefore, here we assume that $\Delta\psi$ is equal to 120 mV for all the considered metabolisms.

Gibbs free energy of a reaction under non-standard condition can be calculated as follow:

$$\Delta G = \Delta G^{\circ} + RT\ln Q \tag{4}$$

Where ΔG° is the Gibbs free energy of a reaction under biochemical standard conditions (25°C, 1 atm, pH 7 and chemical activity of unity (Jin and Kirk, 2018)) and can be calculated by subtracting the sum of Gibbs free energy of formation (ΔG_f°) of substrates from that of products. Q is the reaction quotient. For a hypothetical reaction aA + bB → cC + dD, reaction quotient is equal to:

$$Q = \frac{[C]^c[D]^d}{[A]^a[B]^b} \tag{5}$$

Where [S] is the activity of a reactant/product (S = {A, B, C, D}). Chemical speciation and activity of species are calculated using LLNL Thermodynamic Database (Delany and Lundeen, 1990) and PHREEQC v.3 (pH-REdox-EQuilibrium written in the C programming language (Parkhurst and Appelo, 2013). Activity of S^0 is assumed to be equal to its concentration. Gibbs-Helmholtz equation is used to correct ΔG° for non-standard temperatures:

$$\Delta G_T^{\circ} = \Delta G^{\circ}_{298.15}\left(\frac{T}{298.15}\right) + \Delta H^{\circ}_{298.15}\left(\frac{298.15 - T}{T}\right) \tag{6}$$

Where $\Delta H^{\circ}_{298.15}$ is the enthalpy of a reaction in standard conditions and can be calculated by subtracting the sum of enthalpies of formation of substrates (ΔH_f°) from that of products. The value of ΔG_f° and ΔH_f° for acetate is obtained from Shock (1995), for inorganic species from Shock et al. (1997), and for biomass from Roels (1980).

The rate of biomass (X) formation is given by:

$$\frac{dX}{dt} = (\mu - b)X \tag{7}$$

Where μ[s^{-1}] is the specific growth rate and b[s^{-1}] is the specific maintenance rate. The specific growth rate is linked to respiration rate using growth yield (Y) [mol biomass · (mol ED)$^{-1}$] through the following relationship:

$$\mu = Y\frac{r}{X} \tag{8}$$

Growth yield Y is dependent on ΔG_{cat}, ΔG_{an}, and energy utilization efficiency of organisms (VanBriesen, 2002). In order to study the effect of changes in chemical (variation in species concentrations and pH) and physical (e.g. temperature) conditions, the Gibbs Energy Dynamic Yield Method (GEDYM) of Smeaton and Van Cappellen (2018) is employed:

$$Y = \frac{\alpha\left(\Delta G_{cat}^{\circ}\right)^2 - \beta\Delta G_{cat}^{\circ}\Delta G_{cat}}{\alpha v\left(\Delta G_{cat}^{\circ}\right)^2 - \Delta G_{cat}^{\circ}\left(\beta v\Delta G_{cat} + \alpha\Delta G_{an}^{\circ} + \Delta G_{an}\right) + m\ \Delta G_{cat}\Delta G_{an}^{\circ}} \tag{9}$$

Where α and β are model parameters and equal to -0.0004 and -0.0694 for a broad range of metabolisms including all major EAs, fermentation, methanogenesis and acetogenesis. Smeaton and Van Cappellen only considered hydrogen as the non-organic ED. Note that GEDYM has not been validated for nitrate-reduction, and sulfide-oxidation pathways. However, as the model is valid for all the other metabolisms mentioned above, here we assume that Y for nitrate-reduction and for sulfide-oxidation pathways follows equation 9 as well.

According to equation 7, the biomass growth depends on the thermodynamic dependent terms of Y and F_T. Assuming that microorganisms that derive their energy from the various metabolisms (i) are all present, (ii) have the same kinetic parameters such as v_{max}, K_A and K_D, and (iii) have the same initial biomass concentration (X), terms Y and F_T determine which metabolism proceeds faster. For each metabolism, we consider a set of pH, temperature and concentration of reactants and products in the range observed in petroleum reservoirs and sewer systems, referred to as the base condition.

In order to analyze the temperature effect, the temperature range of

1 to 110°C is evaluated. This is because contrary to sewer systems, where souring occurs in a relatively narrow temperature range, in petroleum reservoirs souring can occur in a relatively broad temperature range, anywhere between the injection temperature (e.g. between 4 to 25°C if North Sea water is injected (CLIMATE-DATA.ORG, 2021) to the reservoir temperature. The temperature of subsurface reservoirs depends on their depth (e.g Willems & Nick 2019). Souring in temperatures higher than 110°C can be ignored as these temperatures preclude microbial activity (Thaysen et al., 2021).

Since chemical compounds depending on temperature and pH can appear in water in various forms, we define the base condition based on the sum of various forms. In the base condition, the water phase is saturated with S^0. Elemental sulfur solubility is calculated by exponential regression of data reported by Kamyshny Jr (2009). Table 3 lists the base condition. C(+4) stands for the sum of carbonate species including carbonic acid (H_2CO_3), bicarbonate (HCO_3^-), carbonate (CO_3^{2-}) and dissolved carbon dioxide ($CO_{2(aq)}$). S(-2) stands for the sum of sulfide species including dihydrogen sulfide (H_2S), hydrogen sulfide (HS^-) and sulfide (S^{2-}). N(-3) stands for the sum of ammonium (NH_4^+) and ammonia (NH_3), and C(0) stands for sum of acetate and acetic acid. We investigate the variations in Y and F_T due to deviations from the base case by changing physical (e.g. temperature) and chemical conditions (e.g. pH and EA concentration).

4. Results

4.1. Variations in Y and F_T for sulfate reduction

4.1.1. Effect of substrate concentration

Fig. 1A and B show Y and F_T of SRM for various ED (acetate) and EA (sulfate) concentrations for the base case. The value of Y changes significantly from 0.4 for EA = ED concentration of 0.028 M, to zero if EA and ED concentration are both less than 10^{-5} M (Fig. 1A). This is because according to equation 4, by reducing the concentration of EA and ED (reactants of SRM catabolic reaction), and ED (reactant of SRM anabolic reaction), respectively, the energy yield of the catabolic reaction ($-\Delta G_{cat}$) decreases and the energy demand of the anabolic reaction (ΔG_{an}) increases. The value of F_T follows a similar trend as Y and decreases from a maximum of around 0.5 when ED and EA are high (0.028 M) to around zero (6×10^{-4} M) when EA and ED are minimal (10^{-10} M, Fig. 1B).

4.1.2. Effect of pH

Fig. 1C demonstrates the effect of pH on Y and F_T of SRM for the base case. In the pH range of 6.6 to 9.8, F_T variations are relatively low and Y shows only a small reduction. Considering the catabolic reaction of SRM and equation 3, F_T depends only on ΔG_{cat}, and ΔG_{cat} depends on the activity of HCO_3^-, HS^- and acetate. Since the activity of these species is relatively pH independent in the pH range of 6.6 to 9.8, ΔG_{cat} and consequently F_T stay relatively constant. The value of Y depends on both ΔG_{cat} and ΔG_{an}. While ΔG_{cat} is relatively constant, in the range of 6.6 to 9.8 due to decrease in NH_4^+ (Fig. 2D) ΔG_{an} increases slightly and this leads to a small reduction in Y (from 0.18 to 0.14). For pH values less than 6.6 and above 9.8 decreases in the activity of HCO_3^- and HS^- result in increases in Y and F_T. For pH values less than 6.6, the decrease in acetate activity cancels out the effect of reduction in HCO_3^- and HS^- activity. Therefore, the slope of F_T (that is, the absolute value of the derivative of F_T) is slightly sharper for pH values higher than 9.8 (0.19 per unit pH) than pH < 6.6 (0.16 per unit pH). For pH values above 9.8, a significant decrease in NH_4^+ activity causes a significant increase in ΔG_{an}. The increase in ΔG_{an} cancels out the decrease in ΔG_{cat} and as a result, the increase in Y values due to an increase in pH above 9.8 (0.04 mol biomass per mol ED) is less than the increase in Y values due to a decrease in pH below 6.8 (0.13 mol biomass per mol ED).

Table 3
Base case condition.

pH	7
T°C	75
Nitrate (mM)	1
Sulfate (mM)	1
C(0) (mM)	1
C(+4) (mM)	8.3
N(-3) (mM)	2.8
S(-2) (mM)	1

4.1.3. Effect of temperature

Fig. 1D illustrates the impact of temperature on Y and F_T of SRM for the base case. Increase in temperature increases the catabolic energy yield ($-\Delta G_{cat}$) as well as ΔG_{an}. While Y decreases slightly (from 0.19 to 0.17 mol biomass per mol ED) as it depends on both ΔG_{cat} and ΔG_{an}, F_T increases by a factor of 2 (from 0.13 to 0.26) since it is only dependent on ΔG_{cat}. Fig. 1E demonstrates how HS^- concentration affects Y and F_T. As HS^- is the product of the catabolic reaction of SRM, the reduction in HS^- increases $-\Delta G_{cat}$, and as a result, both Y and F_T for SRM increase.

4.2. Variations in Y and F_T for nitrate reduction

Various nitrate reduction pathways considered in this study have a sufficiently high $-\Delta G_{cat}$ such that F_T for all of them is equal to one under the conditions for which Y is plotted in Fig. 3.

4.2.1. Effect of substrate concentration

Fig. 3 shows Y for the various nitrate reduction pathways listed in Table 1. For the base case, when the ED concentration increases, growth yield increases for all nitrate reduction pathways. The smallest Y values are associated with $laNRM_1$ and $lhNRM_1$ (maximum 0.12 and 0.34, respectively, Fig. 3A), since these two metabolisms have the lowest $-\Delta G^{'}_{cat}$ (181.96 kJ per mol ED). The value of $\Delta G^{'}_{an}$ for $laNRM_1$ (-82.09 kJ per mol biomass) is the smallest value among $\Delta G^{'}_{an}$ of other nitrate reduction metabolisms listed in Table 1. However, the value of ΔG_{an} for $laNRM_1$ as function of ED concentration (HS^-) varies from -1.1 to 145 kJ per mol biomass. Therefore, while $laNRM_1$ and $lhNRM_1$ have the same ΔG_{cat}, $laNRM_1$ has a lower ΔG_{an} compared to $lhNRM_1$ (41.84 kJ per mol biomass) for ED concentrations greater than 2.4×10^{-5}. A smaller ΔG_{an} for $laNRM_1$ does not cause a higher Y value compared to $lhNRM_1$, as Y depends also on the number of moles of ED (υ) that is utilized in order to synthesize 1 mol of biomass (Smeaton and Van Cappellen, 2018). In $laNRM_1$ metabolism ($\upsilon = 2.1$) only [1- 2.1Y] fraction of the ED (black dashed line in Fig. 3B) is oxidized for energy production, while in $lhNRM_1$ metabolism ($\upsilon = 0$) the ED oxidation only serves for energy production. This can be the reason why Y values of $lhNRM_1$ are higher than those of $laNRM_1$ despite having an equal ΔG_{cat} and a higher ΔG_{an}. The Y values for a given ED concentration (e.g. 10^{-4} M ED) are higher for oNRM (0.77, Fig. 3B) than $laNRM_3$ (0.64, Fig. 3B) since oNRM metabolism has a higher $-\Delta G^{'}_{cat}$ (536.0 kJ per mol ED) than $laNRM_3$ (487.9 kJ per mol ED). The metabolism of oNRM has also a higher $-\Delta G^{'}_{cat}$ compared to $lhNRM_3$. However, the value of υ is equal to 0.525 for oNRM and 0 for $lhNRM_3$. That is, while $-\Delta G^{'}_{cat}$ of oNRM is equal to 536.0 kJ per mol ED, only between 50 to 74% of it (solid line, Fig. 3B) is used for energy production. As a result, the energy produced by oxidation of 1 mol ED in oNRM metabolism is in the range of 57 to 82% of that of $lhNRM_3$ (dotted line in Fig. 3B). Therefore, for a given ED concentration (e.g. 10^{-4} M ED), Y values for $lhNRM_3$ (1.1 mol biomass per mol ED) are higher than for oNRM (0.77). Similar to the plot of Y versus ED concentration (Fig. 3A), the plot of Y versus EA concentration (Fig. 3C) has a positive slope for all nitrate reduction metabolisms. However, the slope of Y versus log of EA concentration is smaller than the slope of Y versus log of ED concentration. For metabolisms with $\upsilon > 0$, this is because ED is present in both catabolic and anabolic reaction, whereas EA is only

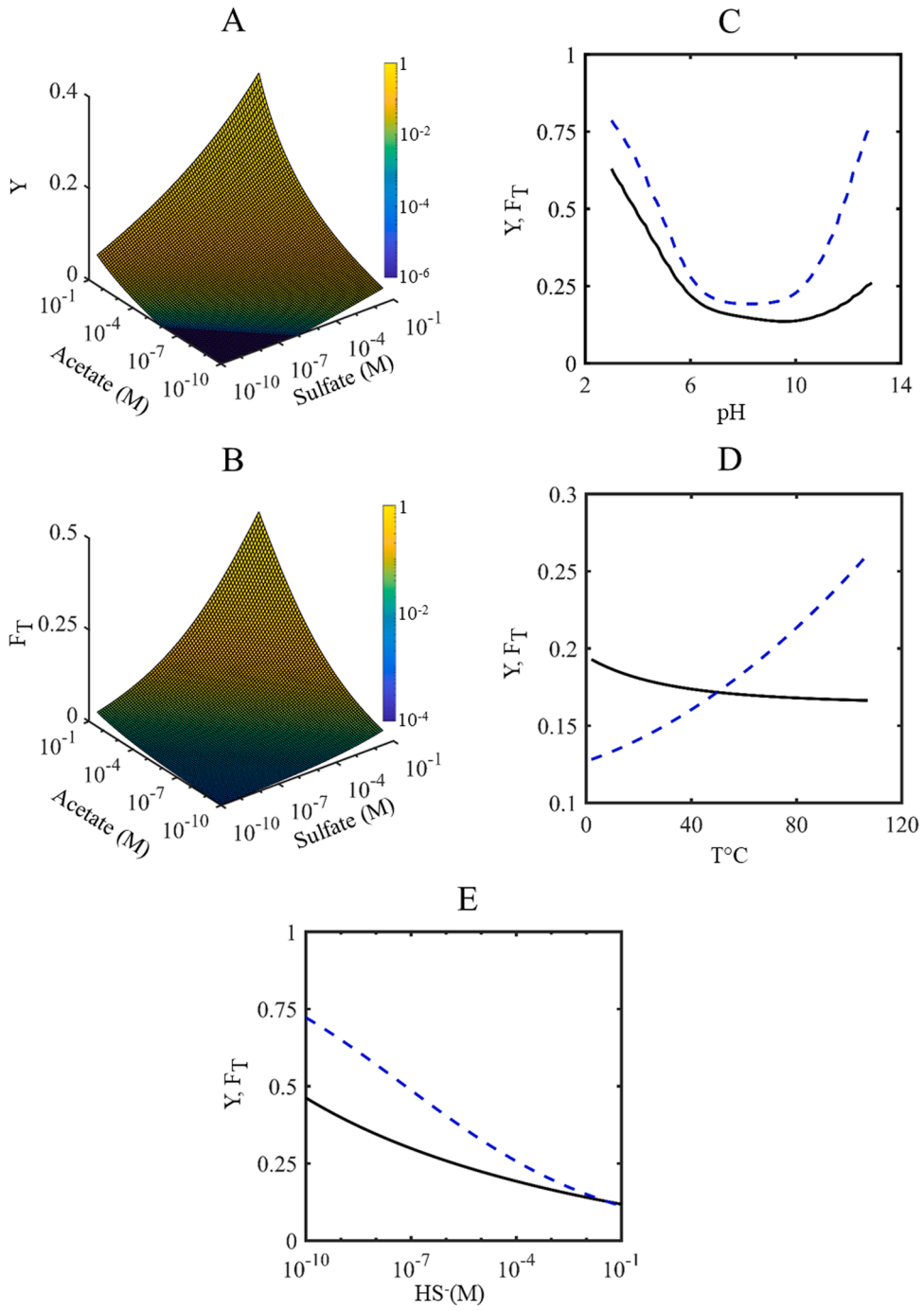

Fig. 1. A) Growth yield (Y) and B) thermodynamic limiting factor (F_T) of SRM calculated using equations 9 and 3, respectively, for various electron acceptor (sulfate) and electron donor (acetate) concentrations, while other influencing parameters such as temperature are equal to the base case. C), D) and E) show the impact of changing pH, temperature and HS^- concentration (from that of the base case) on Y (solid lines) and F_T (dashed lines), respectively.

present in the anabolic reaction. For metabolisms that partially oxidize HS^-, the stoichiometric coefficient of EA is a quarter of the stoichiometric coefficient of ED. Consequently, ΔG_{cat} is a stronger function of ED concentration than of EA concentration.

4.2.2. Effect of pH

Fig. 3D illustrates that in general an increase in pH decreases Y for all the nitrate-reducing metabolisms as they are all proton consuming. However, for low pH values (from 3 to 5), the influence of increasing pH on ΔG_{cat} is canceled out by an increase in HS^- activity (Fig. 2B) for $laNRM_1$ and $lhNRM_1$. The stoichiometric ratio of HS^- to H^+ is bigger for complete oxidation of sulfide compared to the partial oxidation. In consequence, in the pH range of 3 to 5 the impact of an increase in HS^- concentration on ΔG_{cat} of $lhNRM_3$ and $laNRM_3$ is higher than the impact of an increase in pH, leading to an increase in Y. The pH increase effect in oNRM metabolism is canceled out by the increase in acetate concentration (Fig. 2C) in the pH range of 3 to 4. The reduction in Y decreases in pH values higher than 10 for all metabolisms due to reduction of NH_4^+ concentration. For oNRM metabolism, pH values higher than 10 also reduce HCO_3^- concentration. Consequently, the Y value for oNRM levels off relatively at pH 10.

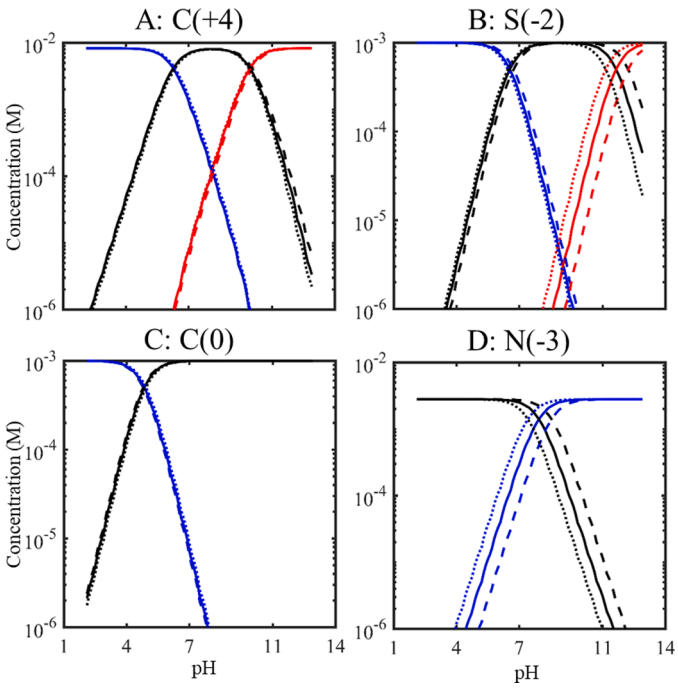

Fig. 2. Variation with pH in concentrations of A) carbonic acid (blue), HCO_3^- (black) and CO_3^{-2} (red), B) H_2S (blue), HS^- (black) and S^{-2} (red), C) acetic acid (blue) and acetate (black) and D) NH_4^+ (blue) and NH_3 (black), predicted by PHREEQC v.3 for three arbitrary temperatures of 50°C (dashed line), 75°C (solid line) and 100°C (dotted line).

4.2.3. *Effect of temperature and sulfate concentration*

Similar to SRM metabolism, temperature influence on Y value of oNRM, $lhNRM_3$, $laNRM_3$ is relatively insignificant (maximum 3.6, 6.0 and 4.0 % change, respectively). The Y values of $lhNRM_1$ and $laNRM_1$ increase significantly from 0.27 to 0.41, and from 0.07 to 0.14, by a reduction in temperature from 110 to 4°C since the decrease in temperature reduces S^0 solubility (Kamyshny Jr, 2009). Among all nitrate reducing metabolisms, Y of $laNRM_3$ and $lhNRM_3$ depend on sulfate concentration. Fig. 3F shows that Y of $laNRM_3$ is greater than Y of oNRM for sulfate concentrations lower than 10^{-5}M.

5. Discussion

5.1. *Importance of taking into account variations in Y and F_T*

SRM activity has caused detrimental consequences such as corrosion and reservoir plugging for seawater injection into oil reservoirs (Youssef et al., 2009). In sewer systems, the H_2S produced by SRM is a major source of odor nuisance (Jiang et al., 2015) and corrosion of concrete sewer pipes (Pikaar et al., 2019). Modeling SRM activity is also essential for mainstream anaerobic digestion technology development (Durán et al., 2020). Microbial sulfate-reduction models have been used to predict the extent of reservoir souring, aiming to minimize the impacts and costs of SRM activity. To the best of our knowledge, in these models Y has been always assumed to be a constant, and the energy that SRM require to maintain transmembrane electric potentials has been ignored (i.e. F_T=1) (e.g. (Cheng et al., 2016; Haghshenas et al., 2012; Veshareh et al., 2021)). Underestimation or overestimation of souring in seawater injection can cause erroneous material design for injection/production wells and surface facilities (Johnson et al., 2017). Additionally, inaccurate estimate of souring does not allow efficient treatment design. For example, in nitrate treatment, over usage of nitrate can lead to accumulation of nitrite, which increases corrosion in production wells (Huang and Zhang, 2006). The growth yield of SRM varies significantly

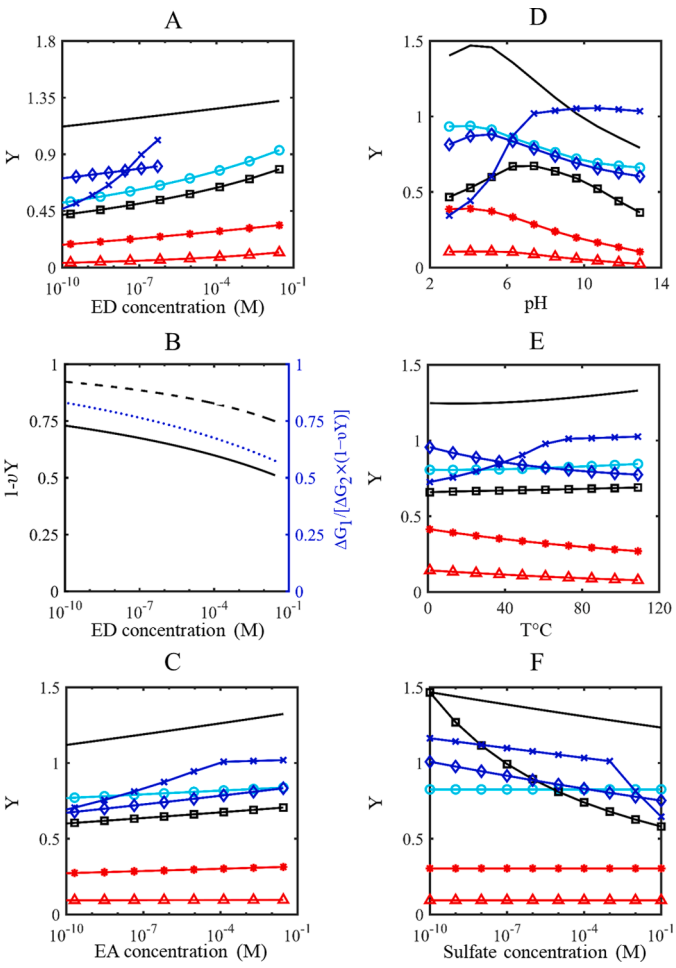

Fig. 3. Growth yield (Y) calculated using equation 9 for organotrophic nitrate reduction (oNRM, circle markers), litho- heterotrophic and autotrophic nitrate reduction coupled to sulfide oxidation to elemental sulfur ($lhNRM_1$, * markers and $laNRM_1$, triangle markers), litho- heterotrophic and autotrophic nitrate reduction coupled to sulfur oxidation to sulfate ($lhNRM_2$, diamond markers and $laNRM_2$, x markers), litho- heterotrophic and autotrophic nitrate reduction coupled to sulfide oxidation to sulfate ($lhNRM_3$, solid line, $laNRM_3$, square markers), for various A) electron donor concentrations (acetate for oNRM, sulfide for $laNRM_1$, $laNRM_3$, $lhNRM_1$ and $lhNRM_3$, and sulfur for $laNRM_2$ and $lhNRM_2$), C) electron acceptor (nitrate) concentrations, D) pH, E) temperature and F) sulfate concentrations. B) Left y-axis, the fraction of electron donor that is used for energy production, right y-axis, the ratio of catabolic energy yield of lithoheterotrophic metabolism to that of lithoautotrophic metabolism, for various electron donor concentrations.

from around 0.33 when the concentration of SRM ED and EA is around the maximum concentration observed in typical seawater flooding processes (0.028 M) (Vigneron et al., 2017), to zero for ED and EA concentrations smaller than 1μM (Fig. 1A). In sewer systems, petroleum reservoirs as well as the biofilm of bioreactors, there is invariably a gradient of substrates. As our results show, the value of Y that controls souring in time and space domains is significantly dependent on the substrate concentrations. Assuming a constant Y value - the value of which depends on the laboratory conditions under which Y has been determined – will thus cause over or underestimation of souring rates in that given time and location. Due to the low exergonicity of SRM catabolic reaction, and depending on the concentration of ED and EA, SRM kinetics will be thermodynamically limited by 60 to around 100% (F_T = 0 to 0.4, Fig. 1B). That is, while assuming a constant Y may over or underestimate souring rate, ignoring F_T will always lead to overestimation of souring. Therefore, accurate souring simulation requires

considering both of these thermodynamic dependent parameters.

Among various environmental conditions, pH is a classical physiological parameter. In order to tolerate acidic or alkaline conditions, microorganisms require special surface properties that protect cells from proton or hydroxide ions (Golyshina and Timmis, 2005; Horikoshi, 1999). Very low or high pH values restrict microbial reactions due to various reasons. For example, at low pH conjugate acids become abundant and diffuse into cell membrane, destabilizing the membrane and dissipating proton motive force (Russell and Dombrowski, 1980). Our results show that in near neutral pH, with an increase in pH, the SRM rate decreases due to reduction in both F_T and Y. The effect of pH on SRM activity has been well studied in the context of wastewater treatment since the pH of waste water can be subject to significant changes due to processes such as fermentation of organics or treatment with alkali (Sharma et al., 2013). Gutierrez et al. (2009) reported that a pH increase from 7.6 to 8.6 and 9.0 reduces the biological sulfate reduction by 30 to 50%.

To further highlight the importance of considering the effect of thermodynamics on souring kinetics, we compare our data with experimental and modelling data published by (Sharma et al., 2014). These authors conducted several batch experiments using a sewer biofilm reactor at various pH values in the range of 4.0 to 9.0 and observed that sulfate reduction rate is maximal at pH 6.3, and decreases when pH deviates from this value. In order to model the pH effect Sharma et al. (2014) used the pH inhibition expression proposed by Angelidaki et al. (1993) for pH values lower than 6.75, and for higher pH values they employed the non-competitive inhibition model of (Siegrist et al., 2002) that is focused on free ammonia. The model developed by Sharma et al. (2014) predicts that souring rate in the range of 6.4 to 8.3 is independent from pH (i.e. is constant), whereas experimental data shows that souring rate decreases with increase in pH in this range (Fig. 4A). The model of Sharma et al. (2014) ignores variations in Y due to pH change and does not take into account any thermodynamic limiting factor. Since the rate of sulfate reduction in the course of Sharma et al. (2014) experiments (Fig. 2 in their work) is constant, the effect of Y variations can be neglected. To evaluate whether the variations in sulfate reduction rate in the pH range of 6.4 to 8.3 is related to changes in F_T, we consider the value of sulfate reduction rate at a reference value and predict other sulfate reduction rates using the following equation:

$$r(pH) = r_{ref}\frac{F_T(pH)}{F_{T_{ref}}} \quad (10)$$

Fig. 4A shows a good agreement between the values predicted using equation 10 and the experimental data. Therefore, considering F_T with $\Delta\psi = 100$ mV can explain changes in sulfate reduction rate in the pH range of 6.4 to 8.3. The strong correlation between F_T and rates is probably due to the minimal impact of physiological parameters as pH values are relatively close to neutral. Note that in pH higher than 7, $-\Delta G_{cat}$ is less than 45 kJ (Fig. 4B), i.e. the model introduced by (Jin and Bethke, 2003) would predict F_T to be equal to zero. Therefore, using the thermodynamic limitation factor proposed by LaRowe et al. (2012) seems to be more appropriate for modeling souring. High pH values also decrease H_2S liquid to gas mass transfer, increasing the total dissolved sulfide (Ganigue et al., 2011). Higher dissolved sulfide concentrations reduce SRM activity not only due to its toxicity (Kushkevych et al., 2019; McCartney and Oleszkiewicz, 1991), but also by reducing the $-\Delta G_{cat}$ of sulfate reduction (Fig. 1E).

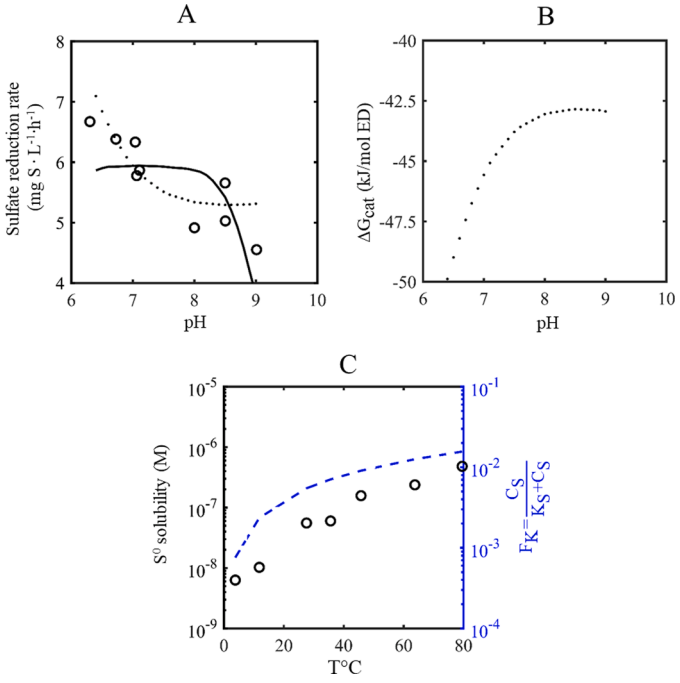

Fig. 4. A) Circle markers, solid line and the dotted line show sulfate reduction rate at different pH values measured by Sharma et al. (2014), modeled by Sharma et al. (2014) and calculated by using equation 10, respectively. B) The Gibbs free energy of catabolic reaction of sulfate reducing microorganisms. C) Left y-axis, circle markers, elemental sulfur (S^0) solubility and right y-axis, dashed line, the kinetic limiting factor (F_K) that takes into account the effect of limitation of electron donor (S^0) on the kinetics of lithotrophic nitrate-reduction, sulfur-oxidation.

5.2. *Is it valid to use the GEDYM for lNRM pathways?*

As mentioned earlier in the methodology section, we assume that GEDYM is valid for estimating the growth yield of lithotrophic metabolisms listed in Table 1. Zeng and Zhang (2005) conducted two batch experiments and measured the growth yield for $laNRM_2$ to be 0.75 and 0.85. The growth yield values calculated in this work using GEDYM (Fig. 3E), matches these experimental values, suggesting that GEDYM holds true also for lithotrophic nitrate reduction based sulfide oxidation.

5.3. *What nitrate-reduction pathway is expected to be faster thermodynamically?*

Assuming (i) a diverse microbial community that can sustain the various nitrate reduction pathways considered in this study, (ii) all community members have the same kinetic parameters and initial biomass concentration, and (iii) the concentration of EA and ED is equal for all metabolisms, $lhNRM_3$ is around two times faster than oNRM pathway, for various physiochemical conditions found in typical petroleum reservoirs. This is in disagreement with the work of Dolfing and Hubert (2017) where except for special conditions such as low temperature, or low acetate to H_2S ratios, oNRM pathway is predicted to prevail. This is because Dolfing and Hubert (2017) consider the pathway with a higher $-\Delta G_{cat}$ as the dominant pathway, while not considering the anabolic reaction. Our results highlights that to find the dominant metabolism among metabolic pathways with high catabolic energy yields (i.e. $F_T = 1$), ΔG_{cat} cannot be used directly to reveal the dominant pathway as it has been used for other metabolisms such as methanogenesis or acetogenesis Jin and Kirk, 2018). Note that while the value of Y allows a quantitative comparison between the rate of two metabolisms in a system at its initial condition, the relationship of respiration rate and Y is not linear and rather exponential (equations 1, 7 and (8). Therefore, a two time higher Y of $lhNRM_3$ compared to that of oNRM can lead to $lhNRM_3$ domination. This is in agreement with various studies available in the literature. Hubert et al. (2003) injected nitrate into a soured bioreactor (sulfide concentration of 12 mM) and observed that despite injection of 25 mM lactate, nitrate reduction was entirely coupled to sulfide oxidation to sulfate. Lambo et al. (2008) showed that lithotrophic reduction of nitrate always preceded organotrophic reduction of nitrate.

Mathioudakis et al. (2006) by conducting experiments on sour waste water samples (sulfide concentration of around 1mM) reported that nitrate reduction is preferentially autotrophic and that heterotrophic nitrate reduction only commenced after sulfide had been completely oxidized. In another study, Okabe et al. (2003) observed that in sewer biofilm experiments, 65% of the H_2S produced by SRM residing in deeper layers of the biofilm was oxidized via lNRM in shallower layers. A similar observation has been reported by Garcia-de-Lomas et al. (2007). Dolfing and Hubert (2017) discussed whether $lNRM_1$ or $lNRM_3$ is expected to be the dominant lNRM pathways by comparing the -ΔG of acetate driven reduction of sulfate and S^0. They proposed that because -ΔG of acetate driven reduction of S^0 is less than acetate driven reduction of sulfate, $lNRM_1$ is the dominant lNRM pathway. They suggested that the dominance of $lNRM_1$ is more likely at lower temperatures, as the differences between -ΔG of acetate driven reduction of S^0 and that of acetate driven reduction of sulfate, increases with temperature. According to our results (Fig. 3), under all studied conditions, lithotrophic sulfide based nitrate reduction is envisaged to be through $lNRM_3$ pathways rather than $lNRM_1$ due to significantly higher Y values (1.6 to 17 times).

5.4. Why does elemental sulfur accumulation occur?

The low growth yield of lithotrophic nitrate reduction coupled to partial sulfide oxidation to sulfur ($laNRM_1$ and $lhNRM_1$) does not imply that nitrate treatment does not cause S^0 production. It merely means that if all the parameters that affect various nitrate reduction pathways are equal, and if oxidation of sulfide to sulfate in a single step is possible, thermodynamically a lower fraction of nitrate reduction is coupled to partial sulfide oxidation and a higher fraction of nitrate is coupled to either complete sulfide oxidation or to oxidation of organic compounds. Veshareh et al. (2021) showed that nitrate treatment by *Desulfobacterium autotrophicum* and a microbial community of a production water enrichment that contained organotrophic nitrate reducing members from *Delta-* and *Gammaproteobacteria* caused S° concentrations of 17 to 22 μM. Jiang et al. (2009) observed that lithotrophic nitrate reduction based sulfide oxidation occurs first by oxidation of sulfide to sulfur ($lNRM_1$), followed by oxidation of sulfur to sulfate ($lNRM_2$). These authors reported that the rate of $lNRM_2$ is 15% of that of $lNRM_1$. Yang et al. (2005) observed that elemental sulfur was the end product of nitrate-based sulfide oxidation. The accumulation of S^0 due to NT has also been reported by Liang et al. (2016). Fig. 3 shows that $lNRM_2$ metabolisms have higher Y values than $lNRM_1$ metabolisms due to significantly higher $-\Delta G_{cat}$ values, i.e. based on thermodynamics the rate of $lNRM_2$ should be higher than that of $lNRM_1$. Fig. 4C demonstrates why $lNRM_2$ can be slower than $lNRM_1$ even though it is thermodynamically more favorable. Sulfur solubility in water is extremely low and increases exponentially with temperature from 6.3×10^{-9} at 4°C to 6.3×10^{-7} M at 80°C (Kamyshny Jr, 2009). By considering 1.7×10^{-5} M (Mora et al., 2015) as the half saturation constant for sulfur, and assuming that the environment is saturated with sulfur, the limiting kinetic term (F_K) will be between 2×10^{-4} and 4×10^{-3} for 4°C and 80°C, respectively. That is, if we ignore the dependency of $lNRM_1$ on any other factor, reduction in temperature from 80 to 4°C, makes $lNRM_1$ 20 times slower merely because of the reduction in S^0 solubility. Therefore, decrease in temperature does not promote S^0 accumulation only by increasing the growth yield of $lNRM_1$ due to an increase in Y, but mainly by reducing S^0 solubility and thereby reducing the rate of S^0 oxidation to sulfate. This explains why in sewer systems where the temperature is relatively low (around ambient temperature) NT is associated with elemental sulfur production as shown by Liang et al. (2016) and Jiang et al. (2009). In reservoir souring processes, S^0 accumulation can be expected to occur mainly in injection tubing and near the well bore area. However, the extent of S^0 accumulation can spread to the production well, provided presence of fractures reduce the travel time between the injection and production wells and thereby reducing the water temperature in the production well. Given the abovementioned temperature dependence of S^0 accumulation, one can conclude that heating injection water can remediate the S^0 related corrosion associated with NT of reservoir souring. Note that in Fig. 4 only the range of 4 to 80°C has been considered because we did not have S^0 solubility data outside this range.

5.5. Single-step sulfide oxidation vs two-step sulfide oxidation

Single step nitrate-based oxidation of sulfide ($lNRM_3$) seems to have both the thermodynamic advantage as well as the kinetic advantage as no elemental sulfur is produced as an intermediate. However, Cui et al. (2019) reported that nitrate reducers that catalyze single step sulfide oxidation to sulfate can only harvest two electrons per nitrate reduced as the nitrate reduction pathways stops at nitrite due to a lack of nitrite reductase. The nitrite produced in the single-step oxidation of sulfide to sulfate is then reduced further by nitrate reducers that oxidize sulfide in two-steps. Therefore, two-step sulfide oxidation has a physiological advantage and is expected to always co-occur with the single-step sulfide oxidation as the organisms involved can reduce nitrite. Cui et al. (2019) showed that compared to the two-step sulfide oxidation, single-step oxidation of sulfide is more sensitive to sulfide, suggesting that the physiological advantage of two-step sulfide oxidation when nitrate treatment is applied increases with the souring level. These observations have implications for souring management where (i) low temperatures, (ii) limited nitrate availability compared to sulfide, or (iii) limited travel time between the injection and production well can cause elemental sulfur accumulation. Therefore, we speculate that souring treatment efficiency by nitrate injection can be improved by (i) early treatment, (ii) increasing temperature, (iii) making sure that stoichiometrically enough nitrate is available for sulfide oxidation, and (iv) reducing injection flow rate (in the case of souring in petroleum reservoirs) such that sufficient time is given to $lNRM_2$ to complete sulfide oxidation (from sulfur to sulfate). Note that half-hearted measures, that include only some of these conditions, may cause even more severe souring problems as for example increase in temperature can increase H_2S emission from the liquid phase to the gas phase.

6. Caveats and future directions

Zhang et al. (2018) have shown that polysulfide formation substantially increases the rate of organotrophic sulfur reduction to sulfide. Qiu et al. (2020) showed that sulfur-based autotrophic denitrification is substantially enhanced due to polysulfide formation. This is why Zhang et al. (2021) introduced polysulfide as an “electron shuttle” that accelerates sulfur oxidation or reduction. Indeed, the polysulfide formation step should not be ignored in the simulation of sulfide/sulfur/sulfate transformations when the exact value of elemental sulfur accumulation or the rate of accumulation is to be evaluated. However, in this study, polysulfide formation from sulfide and elemental sulfur, and polysulfide oxidation to sulfide has been ignored in the sulfur cycle because rather than estimating the pool sizes of the S^0 species, the aim was to predict the likelihood of elemental sulfur accumulation. Future work can validate the proposed methodology in this paper for polysulfide oxidation and study whether the faster oxidation/reduction rates of polysulfide is due to the thermodynamic advantage of this species under varied physiochemical conditions.

7. Conclusions

The key findings of this study can be summarized as follows:

- Growth yield can be used to link the differences in energetics of microbial reactions with their kinetics for metabolisms that have a sufficiently high $-\Delta G_{cat}$ such that thermodynamic limiting factor is equal to one.

- Since the kinetic parameters of souring processes can be substantially affected by thermodynamics, it is essential to couple souring models to a thermodynamic model that takes into account the effect of variations in catabolic energy yield and anabolic energy demand on the metabolism rate.
- Compared to other nitrate reduction pathways such as organotrophic nitrate-reduction, based on the magnitude of growth yield, single-step lithoheterotrophic nitrate reduction driven sulfide-oxidation to sulfate is expected to be the dominant nitrate reduction pathway in sour systems.
- Even though nitrate-reduction, sulfur oxidation to sulfate is thermodynamically expected to be faster than nitrate-reduction, sulfide oxidation to sulfur, it is slower due to the low solubility of elemental sulfur.
- Elemental sulfur accumulation associated with nitrate-reduction driven sulfide-oxidation is prevalent at lower temperatures due to the exponential decrease of sulfur solubility with temperature.

Declaration of Competing Interest

The authors declare that they have no known competing financial interests or personal relationships that could have appeared to influence the work reported in this paper.

Acknowledgements

The research leading to these results has received funding from the Danish Hydrocarbon Research and Technology Centre under the Transformation of Asset Cost program. The three reviewers are thanked for their constructive comments that helped us to improve the manuscript.

References

Agrawal, A., Park, H.s., Nathoo, S., Gieg, L.M., Jack, T.R., Miner, K., Ertmoed, R., Benko, A., Voordouw, G., 2012. Toluene depletion in produced oil contributes to souring control in a field subjected to nitrate injection. Environmental science & technology 46 (2), 1285–1292.
An, S., Tang, K., Nemati, M., 2010. Simultaneous biodesulphurization and denitrification using an oil reservoir microbial culture: effects of sulphide loading rate and sulphide to nitrate loading ratio. Water research 44 (5), 1531–1541.
Angelidaki, I., Ellegaard, L., Ahring, B.K, 1993. A mathematical model for dynamic simulation of anaerobic digestion of complex substrates: focusing on ammonia inhibition. Biotechnology and bioengineering 42 (2), 159–166.
Callbeck, C.M., Agrawal, A., Voordouw, G., 2013. Acetate production from oil under sulfate-reducing conditions in bioreactors injected with sulfate and nitrate. Appl. Environ. Microbiol. 79 (16), 5059–5068.
Cheng, Y., Hubbard, C.G., Li, L., Bouskill, N., Molins, S., Zheng, L., Sonnenthal, E., Conrad, M.E., Engelbrektson, A., Coates, J.D, 2016. Reactive transport model of sulfur cycling as impacted by perchlorate and nitrate treatments. Environmental science & technology 50 (13), 7010–7018.
CLIMATE-DATA.ORG. https://en.climate-data.org/north-america/united-states-of-america/new-york/north-sea-141630/.
Cui, Y.X., Guo, G., Ekama, G.A., Deng, Y.F., Chui, H.K., Chen, G.H., Wu, D., 2019. Elucidating the biofilm properties and biokinetics of a sulfur-oxidizing moving-bed biofilm for mainstream nitrogen removal. Water research 162, 246–257.
Daniels, L., Sparling, R., Sprott, G.D, 1984. The bioenergetics of methanogenesis. Biochimica et Biophysica Acta (BBA)-Reviews on Bioenergetics 768 (2), 113–163.
Delany, J., Lundeen, S., 1990. The LLNL thermodynamical database. Lawrence Livermore National Laboratory. Report UCRL-21658 150.
Dimroth, P., von Ballmoos, C., Meier, T., Kaim, G., 2003. Electrical power fuels rotary ATP synthase. Structure 11 (12), 1469–1473.
Dolfing, J., Hubert, C.R, 2017. Using Thermodynamics to Predict the Outcomes of Nitrate-Based Oil Reservoir Souring Control Interventions. Frontiers in microbiology 8, 2575.
Durán, F., Robles, Á., Giménez, J.B., Ferrer, J., Ribes, J., Serralta, J., 2020. Modeling the anaerobic treatment of sulfate-rich urban wastewater: Application to AnMBR technology. Water Research 184, 116133.
Ganigue, R., Gutierrez, O., Rootsey, R., Yuan, Z., 2011. Chemical dosing for sulfide control in Australia: an industry survey. Water research 45 (19), 6564–6574.
Garcia-de-Lomas, J., Corzo, A., Portillo, M.C., Gonzalez, J.M., Andrades, J.A., Saiz-Jimenez, C., Garcia-Robledo, E., 2007. Nitrate stimulation of indigenous nitrate-reducing, sulfide-oxidising bacterial community in wastewater anaerobic biofilms. Water research 41 (14), 3121–3131.
Golyshina, O.V., Timmis, K.N, 2005. Ferroplasma and relatives, recently discovered cell wall-lacking archaea making a living in extremely acid, heavy metal-rich environments. Environmental microbiology 7 (9), 1277–1288.
Gutierrez, O., Park, D., Sharma, K.R., Yuan, Z., 2009. Effects of long-term pH elevation on the sulfate-reducing and methanogenic activities of anaerobic sewer biofilms. Water research 43 (9), 2549–2557.
Haghshenas, M., Sepehrnoori, K., Bryant, S.L., Farhadinia, M., 2012. Modeling and Simulation of Nitrate Injection for Reservoir-Souring Remediation. SPE Journal 17 (03), 817–827.
Hamilton, T.L., Jones, D.S., Schaperdoth, I., Macalady, J.L, 2015. Metagenomic insights into S (0) precipitation in a terrestrial subsurface lithoautotrophic ecosystem. Frontiers in microbiology 5, 756.
Horikoshi, K., 1999. Alkaliphiles: some applications of their products for biotechnology. Microbiology and molecular biology reviews 63 (4), 735–750.
Huang, C., Li, Z.-l., Chen, F., Liu, Q., Zhao, Y.-k., Zhou, J.-z., Wang, A.-j, 2015. Microbial community structure and function in response to the shift of sulfide/nitrate loading ratio during the denitrifying sulfide removal process. Bioresource technology 197, 227–234.
Huang, Y.H., Zhang, T.C, 2006. Nitrite reduction and formation of corrosion coatings in zerovalent iron systems. Chemosphere 64 (6), 937–943.
Hubert, C., Nemati, M., Jenneman, G., Voordouw, G., 2003. Containment of Biogenic Sulfide Production in Continuous Up-Flow Packed-Bed Bioreactors with Nitrate or Nitrite. Biotechnology progress 19 (2), 338–345.
Hvitved-Jacobsen, T., Vollertsen, J., Nielsen, A.H., 2013. Sewer processes: microbial and chemical process engineering of sewer networks. CRC press.
Jiang, G., Keller, J., Bond, P.L, 2014. Determining the long-term effects of H2S concentration, relative humidity and air temperature on concrete sewer corrosion. Water research 65, 157–169.
Jiang, G., Sharma, K.R., Guisasola, A., Keller, J., Yuan, Z., 2009. Sulfur transformation in rising main sewers receiving nitrate dosage. Water Research 43 (17), 4430–4440.
Jiang, G., Sun, J., Sharma, K.R., Yuan, Z., 2015. Corrosion and odor management in sewer systems. Current opinion in biotechnology 33, 192–197.
Jin, Q., 2012. Energy conservation of anaerobic respiration. American Journal of Science 312 (6), 573–628.
Jin, Q., Bethke, C.M., 2003. A new rate law describing microbial respiration. Applied and Environmental Microbiology 69 (4), 2340–2348.
Jin, Q., Bethke, C.M, 2005. Predicting the rate of microbial respiration in geochemical environments. Geochimica et Cosmochimica Acta 69 (5), 1133–1143.
Jin, Q., Bethke, C.M, 2007. The thermodynamics and kinetics of microbial metabolism. American Journal of Science 307 (4), 643–677.
Jin, Q., Kirk, M.F, 2018. pH as a primary control in environmental microbiology: 1. thermodynamic perspective. Frontiers in Environmental Science 6, 21.
Jin, Q., Roden, E.E, 2011. Microbial physiology-based model of ethanol metabolism in subsurface sediments. Journal of contaminant hydrology 125 (1-4), 1–12.
Johnson, R.J., Folwell, B.D., Wirekoh, A., Frenzel, M., Skovhus, T.L, 2017. Reservoir Souring–Latest developments for application and mitigation. Journal of biotechnology 256, 57–67.
Kadenbach, B., 2003. Intrinsic and extrinsic uncoupling of oxidative phosphorylation. Biochimica et Biophysica Acta (BBA)-Bioenergetics 1604 (2), 77–94.
Kamyshny Jr, A., 2009. Solubility of cyclooctasulfur in pure water and sea water at different temperatures. Geochimica et Cosmochimica Acta 73 (20), 6022–6028.
Kushkevych, I., Dordević, D., Vítězová, M., 2019. Toxicity of hydrogen sulfide toward sulfate-reducing bacteria Desulfovibrio piger Vib-7. Archives of microbiology 201 (3), 389–397.
Lahme, S., Enning, D., Callbeck, C.M., Vega, D.M., Curtis, T.P., Head, I.M., Hubert, C.R, 2019. Metabolites of an oil field sulfide-oxidizing, nitrate-reducing Sulfurimonas sp. cause severe corrosion. Applied and environmental microbiology 85 (3).
Lambo, A.J., Noke, K., Larter, S.R., Voordouw, G., 2008. Competitive, microbially-mediated reduction of nitrate with sulfide and aromatic oil components in a low-temperature, western Canadian oil reservoir. Environmental science & technology 42 (23), 8941–8946.
LaRowe, D.E., Dale, A.W., Aguilera, D.R., L'Heureux, I., Amend, J.P., Regnier, P, 2014. Modeling microbial reaction rates in a submarine hydrothermal vent chimney wall. Geochimica et Cosmochimica Acta 124, 72–97.
Liang, S., Zhang, L., Jiang, F., 2016. Indirect sulfur reduction via polysulfide contributes to serious odor problem in a sewer receiving nitrate dosage. Water research 100, 421–428.
Marietou, A., Kjeldsen, K.U., Røy, H., 2020. Physicochemical and biological controls of sulfide accumulation in a high temperature oil reservoir. Applied Microbiology and Biotechnology 104 (19), 8467–8478.
Mathioudakis, V.L., Vaiopoulou, E., Aivasidis, A., 2006. Addition of nitrate for odor control in sewer networks: laboratory and field experiments. Global NEST Journal 8 (1), 37–42.
McCartney, D., Oleszkiewicz, J., 1991. Sulfide inhibition of anaerobic degradation of lactate and acetate. Water Research 25 (2), 203–209.
Miroshnichenko, M.L., Kostrikina, N.A., Chernyh, N.A., Pimenov, N.V., Tourova, T.P., Antipov, A.N., Spring, S., Stackebrandt, E., Bonch-Osmolovskaya, E.A., 2003. Caldithrix abyssi gen. nov., sp. nov., a nitrate-reducing, thermophilic, anaerobic bacterium isolated from a Mid-Atlantic Ridge hydrothermal vent, represents a novel bacterial lineage. International journal of systematic and evolutionary microbiology 53 (1), 323–329.
Monod, J., 1949. The growth of bacterial cultures. Annual Reviews in Microbiology.
Mora, M., Fernández, M., Gómez, J.M., Cantero, D., Lafuente, J., Gamisans, X., Gabriel, D., 2015. Kinetic and stoichiometric characterization of anoxic sulfide oxidation by SO-NR mixed cultures from anoxic biotrickling filters. Applied microbiology and biotechnology 99 (1), 77–87.

Okabe, S., Ito, T., Satoh, H., Watanabe, Y., 2003. Effect of nitrite and nitrate on biogenic sulfide production in sewer biofilms determined by the use of microelectrodes. Water science and technology 47 (11), 281–288.
Parkhurst, D.L., Appelo, C., 2013. Description of input and examples for PHREEQC version 3: a computer program for speciation, batch-reaction, one-dimensional transport, and inverse geochemical calculations. US Geological Survey.
Pikaar, I., Flugen, M., Lin, H.-W., Salehin, S., Li, J., Donose, B.C., Dennis, P.G., Bethke, L., Johnson, I., Rabaey, K., 2019. Full-scale investigation of in-situ iron and alkalinity generation for efficient sulfide control. Water research 167, 115032.
Qiu, Y.-Y., Zhang, L., Mu, X., Li, G., Guan, X., Hong, J., Jiang, F., 2020. Overlooked pathways of denitrification in a sulfur-based denitrification system with organic supplementation. Water research 169, 115084.
Roels, J., 1980. Application of macroscopic principles to microbial metabolism. Biotechnology and Bioengineering 22 (12), 2457–2514.
Russell, J.B., Dombrowski, D., 1980. Effect of pH on the efficiency of growth by pure cultures of rumen bacteria in continuous culture. Applied and Environmental Microbiology 39 (3), 604–610.
Schmitt, G., 1991. Effect of elemental sulfur on corrosion in sour gas systems. Corrosion 47 (4), 285–308.
Sharma, K., Derlon, N., Hu, S., Yuan, Z., 2014. Modeling the pH effect on sulfidogenesis in anaerobic sewer biofilm. water research 49, 175–185.
Sharma, K., Ganigue, R., Yuan, Z., 2013. pH dynamics in sewers and its modeling. Water research 47 (16), 6086–6096.
Sharma, K.R., Yuan, Z., de Haas, D., Hamilton, G., Corrie, S., Keller, J., 2008. Dynamics and dynamic modelling of H2S production in sewer systems. Water Research 42 (10-11), 2527–2538.
Shock, E.L., 1995. Organic acids in hydrothermal solutions: Standard molal thermodynamic properties of carboxylic acids and estimates of dissociation constants at high temperatures and pressures. American Journal of Science 295 (5), 496–580.
Shock, E.L., Sassani, D.C., Willis, M., Sverjensky, D.A, 1997. Inorganic species in geologic fluids: correlations among standard molal thermodynamic properties of aqueous ions and hydroxide complexes. Geochimica et Cosmochimica Acta 61 (5), 907–950.
Siegrist, H., Vogt, D., Garcia-Heras, J.L., Gujer, W., 2002. Mathematical model for meso- and thermophilic anaerobic sewage sludge digestion. Environmental science & technology 36 (5), 1113–1123.
Smeaton, C.M., Van Cappellen, P., 2018. Gibbs Energy Dynamic Yield Method (GEDYM): Predicting microbial growth yields under energy-limiting conditions. Geochimica et Cosmochimica Acta 241, 1–16.
Thaysen, E.M., McMahon, S., Strobel, G.J., Butler, I.B., Ngwenya, B.T., Heinemann, N., Wilkinson, M., Hassanpouryouzband, A., McDermott, C.I., Edlmann, K., 2021. Estimating microbial growth and hydrogen consumption in hydrogen storage in porous media. Renewable and Sustainable Energy Reviews 151, 111481.
Toei, M., Gerle, C., Nakano, M., Tani, K., Gyobu, N., Tamakoshi, M., Sone, N., Yoshida, M., Fujiyoshi, Y., Mitsuoka, K., 2007. Dodecamer rotor ring defines H+/ATP ratio for ATP synthesis of prokaryotic V-ATPase from Thermus thermophilus. Proceedings of the National Academy of Sciences 104 (51), 20256–20261.
VanBriesen, J.M., 2002. Evaluation of methods to predict bacterialyield using thermodynamics. Biodegradation 13 (3), 171–190.
Veshareh, M.J., Ayatollahi, S., 2019. Microorganisms' effect on the wettability of carbonate oil-wet surfaces: implications for MEOR, smart water injection and reservoir souring mitigation strategies. Journal of Petroleum Exploration and Production Technology 1–12.
Veshareh, M.J., Kjeldsen, K.U., Findlay, A.J., Nick, H.M., Røy, H., Marietou, A., 2021. Nitrite is a more efficient inhibitor of microbial sulfate reduction in oil reservoirs compared to nitrate and perchlorate: A laboratory and field-scale simulation study. International Biodeterioration & Biodegradation 157, 105154.
Veshareh, M.J., Nick, H.M, 2019. A sulfur and nitrogen cycle informed model to simulate nitrate treatment of reservoir souring. Scientific reports 9 (1), 7546.
Veshareh, M.J., Nick, H.M, 2021a. Biased samples to study reservoir souring processes: a numerical analysis. Journal of Cleaner Production.
Veshareh, M.J., Nick, H.M, 2021b. Growth kinetic and transport of mixed microbial cultures in subsurface environments. Advances in Water Resources, 103929.
Vigneron, A., Alsop, E.B., Lomans, B.P., Kyrpides, N.C., Head, I.M., Tsesmetzis, N., 2017. Succession in the petroleum reservoir microbiome through an oil field production lifecycle. The ISME Journal.
Willems, C.J.L., Nick, H.M., 2019. Towards optimisation of geothermal heat recovery: An example from the West Netherlands Basin. Applied energy 247, 582–593.
Yang, W., Vollertsen, J., Hvitved-Jacobsen, T., 2005. Anoxic sulfide oxidation in wastewater of sewer networks. Water science and technology 52 (3), 191–199.
Youssef, N., Elshahed, M.S., McInerney, M.J, 2009. Microbial processes in oil fields: culprits, problems, and opportunities. Advances in applied microbiology 66, 141–251.
Zhang, L., Qiu, Y.-Y., Zhou, Y., Chen, G.-H., van Loosdrecht, M.C., Jiang, F., 2021. Elemental sulfur as electron donor and/or acceptor: Mechanisms, applications and perspectives for biological water and wastewater treatment. Water Research, 117373.
Zhang, L., Zhang, Z., Sun, R., Liang, S., Chen, G.-H., Jiang, F., 2018. Self-accelerating sulfur reduction via polysulfide to realize a high-rate sulfidogenic reactor for wastewater treatment. Water research 130, 161–167.